Jurnal Kejuruteraan 38(2) 2026: 715-725
https://doi.org/10.17576/jkukm-2026-38(2)-20

Assessing Geohazard Risk on a Weathered Sedimentary Rock Slope Using Photogrammetry Approach

Fatin Nur Ashikin Ab Aziz[a], Aniza Albar[a*], & Mohd Mustaqim Mohd Nordin[b]

[a]*Faculty of Civil Engineering, Universiti Teknologi MARA Shah Alam, 40450, Shah Alam, Selangor, Malaysia,*

[b]*Faculty of Civil Engineering, Universiti Teknologi MARA Pahang, 26400 Bandar Tun Abdul Razak, Pahang, Malaysia.*

[*]*Corresponding author: anizaalbar@uitm.edu.my*

Received 24 June 2025, Received in revised form 30 October 2025
Accepted 30 November 2025, Available online 30 March 2026

ABSTRACT

Weathered sedimentary rock slopes must be in stable condition to reduce the risks and disasters, especially when there are critical infrastructures in proximity. Risk assessment, exposure analysis, vulnerability analysis, hazard identification, mapping, and zoning are the factors that are impacted by the instability of the rock slope in the geohazard vulnerability assessment. This study aims to determine the weathering grade, build high-density 3D models using unmanned aerial vehicle (UAV)-based photogrammetry, identify anisotropic planes based on kinematic analysis and analyse geohazard risk and vulnerability index. The results demonstrated that unfavourable discontinuity orientations and weathering lead to wedge failure at Location A and planar failure at Locations B and C as the primary mechanisms on the weathering grade III sedimentary rock. Infrastructure risks are categorised as low to moderate by vulnerability assessments, where roads and buildings benefit from moderate slope angles and the presence of the drainage systemsalong the retaining structures, with the index value ranging from 0.24 to 0.29. Additionally, forecasts from Agisoft Metashape, CloudCompare, and Stereonet software are aligned with observed failures in the field, such as wedge failure forecasted by kinematic analysis and was confirmed upon observation at Location A. By providing information through vulnerability and risk assessments to support infrastructure development and catastrophe mitigation, the integration with UAV also provides a comprehensive alternative to conventional slope stability analysis techniques for data acquisition in the field.

Keywords: Weathered sedimentary rock slope; unmanned aerial vehicle (UAV); photogrammetry; discontinuity characterisation; and geohazard vulnerability and risk analysis

INTRODUCTION

Among the most frequent and hazardous natural calamities are rockslides, particularly in regions with steep interbedded sedimentary rock slopes. These slopes are susceptible to structural weaknesses such as bedding planes, faults, and joints, which are made up of alternating layers of hard and soft rocks, as well as differential weathering and erosion. These characteristics make slope instability a significant area of research in geotechnical engineering since they raise the possibility of slope instability. These slopes' stability directly affects the surrounding infrastructure's safety and the avoidance of possible failures.

Structural discontinuities such as joints and faults play an important role in slope failures by determining the mode of failure. The orientation and spacing of these discontinuities affect failure mechanisms like wedge sliding, planar sliding, and toppling sliding (Hoek et al. (2007); Bell (2007); A. Johari (2015); Tang et al. (2016); M. Amini et al. (2018). These elements can cause unanticipated and disastrous slope failures, endangering infrastructure and public safety, if they are not properly analysed and their effects are lessened. In addressing the slope stability of weathered Kenny Hill slopes, it requires a multifaceted understanding of geotechnical parameters, weathering impacts and good predictive assessments (Hamzah & Yusof 2022); Azarafza et al. 2022).

Employing photogrammetry data for stability analysis of interbedded sedimentary rock slopes is a crucial application in geotechnical engineering. According to Tannant (2015); Frodella et al. (2021); Albarelli et al.

(2021), photogrammetry is one of the methods that provides a quick and economical means of obtaining the necessary information for the geotechnical characterisation and hazard assessment of steep rock faces. However, Tuckey and Paul (2016) demonstrated that this approach facilitates slope stability assessments by enabling the thorough mapping of rock discontinuities in regions that are normally unavailable for traditional mapping approaches. Furthermore, Li (2024) highlighted the benefits of unmanned aerial vehicle (UAV) photogrammetry, pointing out that it can overcome data-collecting difficulties in rock slope stability studies, allowing for more thorough investigations.

The photogrammetry approach to evaluating rock slope stability has been proven in numerous research studies, demonstrating its efficacy in analysing 2D and 3D rock slope stability using approaches like the Limit Equilibrium Method, according to the study by Nagendran et al. (2019). The usefulness of photogrammetry in geotechnical evaluations has also been highlighted by the application of 3D-DDA in conjunction with UAV-Laser Scanner (UAV-LS) photogrammetry for stability investigation of blocky rock mass slopes (Liu et al. 2019). Additionally, the multistep rocky slope stability analysis based on unmanned aerial vehicle photogrammetry was successfully detailed in Wang (2019), which has shown potential in improving our understanding of slope stability dynamics. Ren and Meng (2022) established composite sliding surface stability methods for layered slopes by using numerical simulations to investigate the mechanical reaction mechanisms and sliding surface features in the setting of interbedded sedimentary rock slopes. Additionally, studies on the stability analysis of anti-inclined rock slopes with soft-hard interbedded rock have been conducted, offering theoretical backing for the analysis of such intricate slope configurations (Guo et al. 2023).

A vital component of guaranteeing the security and stability of communities and infrastructure in regions vulnerable to geological hazards is the evaluation of geohazard vulnerability on rock slopes. Numerous research studies provide insightful information on the methods and variables affecting these evaluations. Albar and Mohd-Nordin (2022) have examined the usage of rock mass categorisation systems as a crucial method for assessing the stability of rock slopes. By measuring the stability of rock slopes according to a variety of geological factors, these systems, like the Slope Mass Rating (SMR), are essential in determining the vulnerability to geohazards. Furthermore, it was demonstrated by Mao et al. (2023) that the incorporation of artificial intelligence (AI) applications has demonstrated potential in improving the study of rock slope instabilities, leading to quicker and more precise evaluations.

In addition, according to Zhang et al. (2023), the vulnerability of rock and soil mass movement geological hazards in particular areas, like Xuanwei, China, emphasises the significance of carrying out in-depth research to prevent and manage such hazards effectively. Developing mitigation strategies and emergency response plans requires an understanding of the geological features and environmental factors that contribute to slope failures and rockfalls, especially in locations like abandoned limestone quarries that are vulnerable to geohazard events (Hussin et al. 2022). According to Li et al. (2022) and Jia et al. (2021), the intricacy of evaluating and controlling rock slope vulnerabilities is further underscored by the influence of topographical features, geological settings, and external influences such as climate change on geohazard susceptibility. Finally, He et al. (2023) proposed that incorporating these many elements into risk assessment frameworks, for example, considering development inhomogeneity in mountainous regions, can enhance decision-making and offer a thorough grasp of geohazard hazards.

This study approaches innovative methods for a comprehensive analysis of geohazard risk assessment with the integration of UAV equipment. This study aims to determine the weathering grade of the sedimentary rock, identify the geological features of interbedded sedimentary rock slopes and anisotropic planes based on kinematic analysis and analyse the geohazard vulnerability and risk by referring to the guideline established by the Construction Research Institute of Malaysia (CREAM) and the industries' joint technical committee (2020). By integrating UAV-SfM with the guidelines, failure prediction will be improved, and early warnings can be transmitted to the appropriate units for mitigating actions.

METHODOLOGY

ROCK SLOPE CHARACTERIZATION

The rock slope was situated at 3°11'56" N, 101°27'35" E, inside the Puncak Alam Campus of Universiti Teknologi (UiTM) MARA Selangor Branch, as shown in Figure 1.

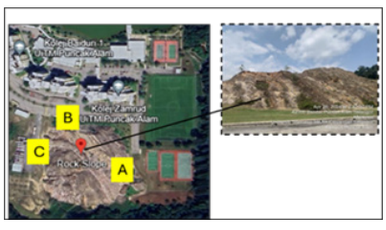

FIGURE 1. Site study

On the sedimentary rock slope from the Kenny Hill Formation, sandstone and shale strata are interbedded. Due to the presence of fossil assemblages such as radiolarians and ammonoids in the layers, the Kenny Hill Formation has been geologically dated to the Early Carboniferous-Permian period (Baioumy et al. 2020). Additionally, a study by Abbas et al. (2023) effectively established an empirical connection to estimate shear strength based on direct shear testing, validating the fact that soil properties vary depending on the parent lithology, which is shale (phyllite) and weathered sandstone (quartzite).

Near the rock slope, few infrastructures were constructed. As seen in Figure 2, four sport courts were located at Location A, two blocks of student hostels at Location B, while the bus depot was located at Location C. The distances were roughly 15 metres for the nearest sport court, 32 metres (Kolej Baiduri), 18.5 metres (Kolej Zamrud), and 10 metres for the bus depot from the toe of the rock slope.

FIGURE 2. Distance of infrastructures to the rock slope (a) Location A; Sport courts; (b) Location B; Kolej Baiduri; (c) Location B; Kolej Zamrud; (d) Location C: Bus depot

As shown in Figure 3, the discontinuity survey and the photogrammetry technique utilising an unmanned aerial vehicle (UAV) were both carried out on-site for data gathering. The activities involved in discontinuity surveys were establishing a scanline, a surface strength test by using a Schmidt Rebound Hammer and measurement of dip angle and dip direction of the discontinuities by using a geological compass.

FIGURE 3. Discontinuities survey and photogrammetry method (a) Distance measurement; (b) Surface strength measurement; (c) Orientation of discontinuities measurement; (d) Flight path mode of drone

DIGITAL IMAGE PROCESSING AND KINEMATIC ANALYSIS

To create 3D models of the rock slope, images from the UAV were loaded into the Agisoft Metashape program. Figure 4 shows the steps involved in picture processing and the workflow for 3D reconstruction.

Cloud Compare, an open-source application, was then used to import the photogrammetric point cloud data. The Compass plugin was used in CloudCompare in accordance with Singh et al. (2022) methodology. Figure 5 illustrates the process for utilising the Compass plugin in CloudCompare to derive geological planes.

Kinematic analysis was carried out using Stereonet software following the extraction of the discontinuity data, which included dip angle and dip direction. Several techniques for creating stereographic projections, which are crucial for locating major discontinuity sets, were covered by Obregon and Mitri (2019). Discontinuity orientations can be shown in the software as big circles, dip vectors, planes, or poles. Figure 6 illustrates the process used in Stereonet software to project the rock slope's mechanism of failure.

VULNERABILITY ASSESSMENT AND RISK ANALYSIS

Risk and vulnerability were evaluated using a semi-qualitative approach. Using hazard and vulnerability data, a risk matrix was developed to categorise and rank risk zones for key infrastructures close to the slope. The development of geohazard maps and vulnerability indices yielded crucial data for risk reduction and management plans. The guidelines from CIDB (2020) have been referred to as evaluating the risk and vulnerability of a critical facility. A cluster indicator and its sub-indicators, including the vulnerability of critical infrastructure (C), the surrounding environment (E), the intensity of landslides (I), and people (P), were chosen as part of the exposure analysis on the critical infrastructure (CI). Low and strong influence to enhance vulnerability are shown by the tolerance of vulnerability index's 0.1 and 1.0 sequences, respectively.

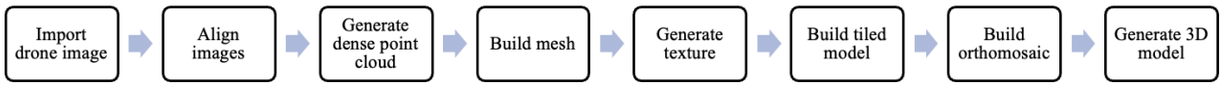

FIGURE 4. Image processing and 3D reconstruction in Agisoft Metashape software

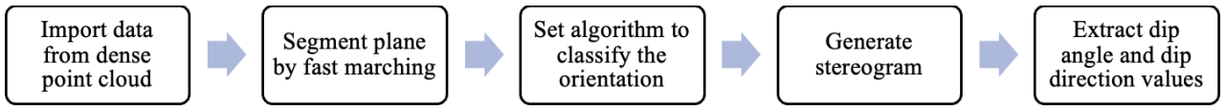

FIGURE 5. Discontinuity extraction using compass plugin in CloudCompare software

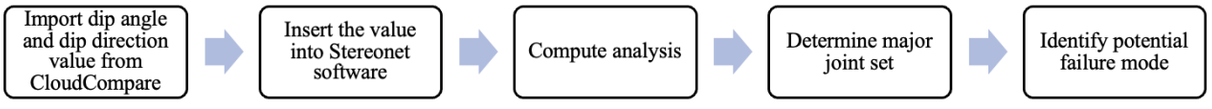

FIGURE 6. Workflow of identification of major discontinuity sets in Stereonet software

RESULTS AND DISCUSSION

WEATHERING GRADE

Rebound values from the Schmidt Rebound Hammer test have also been used to evaluate the rock slope surface's strength. Locations A, B, and C had average rebound numbers of 28, 32, and 21, respectively. According to the weathering classification by Mohamad et al. (2022), the weathering grade from all locations was grade III, which is moderately weathered.

The moderately weathered sedimentary rock at position C is delicate and breakable with hands and a geological hammer, as seen in Figure 7. More than half of the rock material breaking down into soil is categorised as highly worn sedimentary rock. Advanced weathering decreased the rock's shear strength and made it more prone

to failure, especially in the weak shale layers. A light-coloured rock surface means that darker minerals have leached or that oxide coatings or clay minerals have formed because of weathering.

FIGURE 7. Light-coloured rock surface shows the moderately weathered condition at Location C

3D MODEL OF ROCK SLOPE

The Agisoft Metashape program was used to import photos taken from photogrammetry data. Figure 8 displays the UAV-captured image of the rock slope, and Figure 9 displays the high-resolution 3D model of site A. The generated 3D model was aligned with the study by Nagendran et al. 2019; Wang et al. 2019; Ren and Meng 2022; Guo et al. 2023 despite the different 3D model programs that were tilized in each study. In addition, the ruler in the software was used to measure the slope geometry, including slope height and width.

FIGURE 8. UAV-captured image by using drone

FIGURE 9. A 3D model of Location A created with Agisoft Metashape software

KINEMATIC ANALYSIS

The discontinuity parameters, dip angle, and dip direction were extracted using the CloudCompare software in the photogrammetry method. The extraction of planes at Location A is depicted in Figure 10, where the green-coloured zone shows the detection of weakness planes such as joints and faults on the surface of the rock slope. The values of dip angle and direction are then extracted and transferred to the Excel file and further used in kinematic analysis (Nagendran et al. 2019).

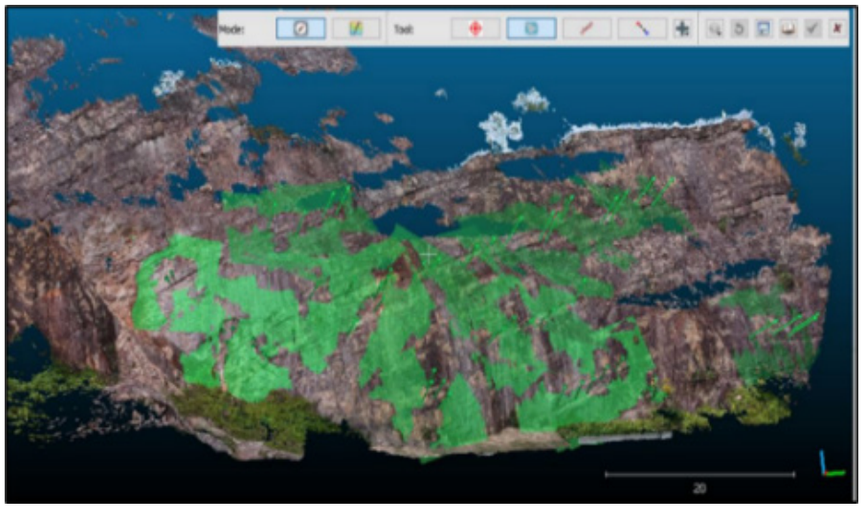

FIGURE 10. Utilizing a CloudCompare software for plane extraction at Location A

Table 1 displays the on-site conditions for Locations A, B, and C as well as the outcomes of stereographic projection using Stereonet. The projection of modes of failure was consistent with the study by Obregon and Mitri (2019); Nagendran et al. (2019); and Singh et al. (2022), which highlights the importance of accurate joint orientation in predicting slope failure risks.

TABLE 1. Stereographic projection and on-site failure

Location	Stereographic projection	On-site condition
A	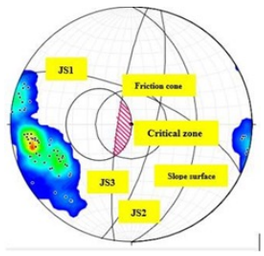	
B	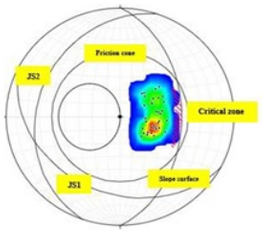	
C	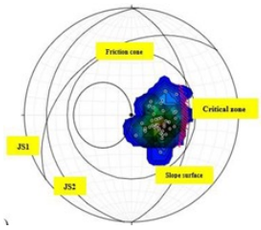	

KINEMATIC ANALYSIS OF LOCATION A

For the rock slope surface at Location A, 63 values of dip angle and dip direction were retrieved and entered into the Stereonet program. The contoured pattern of discontinuity sets shows the outcomes of the evaluation of the findings of three significant joint sets of discontinuity patterns. A critical zone developed in the friction cone and slope face as a result of the wedge failure. A line of junction was generated by two intersecting planes (JS1 and JS2); this line plunges steeper than the slope's plummet and trends toward the slope's face direction. Significant dip/dip projections of 18°/258° are involved in wedge failure at point A. The on-site observation, which shows the new wedge failure and the continuous instability of the rock slope, confirms this, as seen in Table 1.

KINEMATIC ANALYSIS OF LOCATION B

At Location B, the rock slope's dip angle and dip direction had 35 values. On the contoured pattern of discontinuity sets, the results of the evaluation of two significant joint sets of discontinuity patterns are displayed. JS1, the point east on the slope surface, was where the friction cone and slope face intersected. Planar failure can happen when a plane dips out of the slope face and crosses the slope inside the friction cone but at a lower angle than the slope itself. Consequently, planar failure with large dip/dip projections of 68°/119° takes place at Location B. It has also been possible to observe the actual slope face where planar failure has occurred. The material that slid along the planar discontinuities has been displaced, as seen in the red circle in Table 1. Given the orientation and dip direction found in the Stereonet software, the failure is easily observable. Similar circumstances could lead to more failures, particularly when there are outside triggers like intense rain.

KINEMATIC ANALYSIS OF LOCATION C

For the rock slope at Location C, the dip angle and dip direction had 42 values. The contoured pattern of discontinuity sets shows the outcomes of the evaluation of the findings of three significant joint sets of discontinuity patterns. The point east on the slope surface was JS1, where the friction cone and slope face intersected.

A plane that dips out of the slope face and crosses the slope within the friction cone at a lower angle than the slope itself may experience planar failure. Consequently, Location C experiences planar failure with large dip/dip projections of 81°/221°. A surface that is worn and broken, with steep bedding planes and obvious discontinuities, as seen in Table 1. Planar sliding along the bedding planes is possible, as seen by the steep dip and exposed discontinuities.

The rock mass is weaker and more likely to slide because of weathering. Additionally, the material from a prior breakdown is reflected in the buildup of loose debris at the slope's toe.

GEOHAZARD RISK ASSESSMENT

In geohazard risk assessment, only locations B and C fulfilled the requirements highlighted in the guideline from CIDB (2020). The guideline focuses on the risk of the slope towards these critical infrastructures, such as residential or building areas, roads, dams and utilities, specifically power lines. Thus, this study aims to assess both hostels and road pavements which are located near to Locations B and C, respectively.

VULNERABILITY CLASSES FOR LOCATION B

Both hostels are structures that are susceptible to rockslides. Given that the site is in an urban area, the population density is classified as high. Both hostels are located 18.5 and 32 metres away from the rock slope, respectively.

For both residential blocks, the Vulnerability Index (VI) value was 0.241, indicating a low degree of vulnerability. The structure is considered stable; there are not many visible wall fractures, and there is a slight chance that anyone inside the blocks will sustain minor injuries if the rock slope fails.

Additionally, two retaining walls with horizontal drains were built at the toe of the slope, as illustrated in Figure 11. As the kinematic analysis projects the possible planar failure in this location, the retaining walls were functioning to resist the lateral stresses exerted by the rock mass and manage groundwater levels, supporting the findings by Du et al. (2023) and Bakhshayesh et al. (2023).

FIGURE 11. Double retaining walls with horizontal drains at Location B

VULNERABILITY CLASSES FOR LOCATION C

In Location C, the road is constructed roughly ten metres from the toe of the slope. Alongside the road is a bus depot that can accommodate up to 14 university buses at once.

The road segment has a very low vulnerability to rock slope failure threats, according to the VI of 0.289. The result of the land use planning and risk management techniques was the establishment of a bus depot next to the rock slope. The main goal is to reduce the risk to human life while allowing for some possible property damage (Lamessa & Meten, 2021). Damage to the bus depot's smaller structures and buses, which are replaceable assets, would be the main cause of the loss in the rock slope failure. Furthermore, due to less human activity in bus depots, particularly during off-peak hours when the buses are not in service, there is a lower chance of fatalities.

Understanding the possible effects of risks on infrastructure, the environment, and the population requires the use of risk analysis. To determine an overall danger of the structures, the clusters are combined to provide a VI. The findings help stakeholders prioritise resources for emergency response and mitigation and identify high-risk locations that align with the findings from Liu et al. 2021. Ensuring public safety, safeguarding vital infrastructure, and preserving service and transportation continuity are vital. The elements of roads and buildings that can support risk analysis are listed in Table 2.

TABLE 2. Road and building aspects in risk analysis

Aspect	Building	Road
Vulnerability Index (VI)	0.241	0.289
Risk Level	Low to Moderate	Low to Moderate
Dominant Factor Risk	Rockslide Intensity (I)	Rockslide Intensity (I)

The risk of rock slope failure is influenced by its surroundings since they can identify possible effects on infrastructure, economic activity, and human life, as highlighted by Liu et al. 2021. Exposure to possible rock slope failure tends to rise due to the everyday presence of personnel, students, and public transit. Building and facility damage could disrupt the routine and result in financial losses.

CONCLUSION

The weathering grade obtained for all three locations was grade III, which is moderately weathered. The observation

on site was aligned with the field measurements of the strength of the rock slope surface.

Agisoft Metashape software was used to identify the geological characteristics of the weathered sedimentary rock slope and to create high-resolution 3D models of the slope. The software produced a dataset for additional research by capturing extensive information about bedding planes, fault structures, joint orientations, and slope geometry.

Critical anisotropic planes, such as bedding planes, joint sets, and fault zones, were then found by kinematic analysis to be possible sliding surfaces. The 3D point cloud data produced by Agisoft Metashape was processed using CloudCompare software. All measurements of bedding planes, slope angles, and joint orientations are made by this software. Stereonet was also used to assess possible failure modes and locate important anisotropic planes. Plotting joint sets and bedding planes on stereographic projections was done by integrating data from CloudCompare. Planar failure is predicted to happen along steeply sloping bedding planes parallel to the slope face at locations B and C, according to the kinematic analysis. On the other hand, where the plunge direction coincides with the slope at Location A, wedge failure could occur at the junctions of joint sets and bedding planes.

Lastly, regions with different risk levels were indicated by the Vulnerability Index (VI). The VIs for locations B and C were 0.241 and 0.298, respectively. Critical infrastructure susceptibility, the surrounding environment, landslide intensity, and population exposure were all evaluated to decide the zoning. Because of their proximity to possible failure zones and high rockslide intensity, the evaluation found that both hostels, which are near to the slope toe, exhibit low to moderate risk. Although the road alignment at the slope toe is equally in low- to moderate-vulnerability zones, they nevertheless need to be monitored regularly and have their slope drainage improved.

It is recommended to improve the UAV-SfM processing workflow for analytics procedures like manually cleaning the rock faces to separate vegetation from rock. In addition, it is suggested that the study creates the risk zonation to improve the predictive evaluation of vital facilities close to rock slopes and enable the implementation of appropriate mitigation strategies.

ACKNOWLEDGEMENT

The authors would like to thank Universiti Teknologi MARA Shah Alam and Universiti Teknologi MARA Puncak Alam for providing laboratory facilities and supporting this research.

DECLARATION OF COMPETING INTEREST

None.

REFERENCES

Abbas, H., Mohamed, Z., Taher, M., Kudus, S., Salman, M. & Ghaltan, H. 2023. Shear strength characteristics of weathered jointed Kenny Hill interbedded formation for cylindrical specimens under direct shear test. *International Journal of Applied Mechanics and Engineering* 28(2): 1-12. https://doi.org/10.59441/ijame/168938

Abdullah, C. H. & Jaapar, A. R. 2020. *Guideline for landslide vulnerability assessment and risk analysis for critical infrastructure (CI) in Malaysia*. Construction Research Institute Malaysia, hlm. 1-55.

Albar, A. & Mohd-Nordin, M. 2022. Slope mass rating (SMR) classification for rock slope stability and geohazard vulnerability assessment. *International Journal of Integrated Engineering* 14(5). https://doi.org/10.30880/ijie.2022.14.05.006

Albarelli, D., Mavrouli, O. & Nyktas, P. 2021. Identification of potential rockfall sources using UAV-derived point clouds. *Bulletin of Engineering Geology and the Environment* 80(8): 6539-6561. https://doi.org/10.1007/s10064-021-02306-2

Amini, M., Ardestani, A. & Khosravi, M. H. 2017. Stability analysis of slide-toe-toppling failure. *Engineering Geology* 228: 82-96.

Azarafza, M., Hajialilue-Bonab, M. & Derakhshani, R. 2022. A novel empirical classification method for weak rock slope stability analysis. *Scientific Reports* 12(1). https://doi.org/10.1038/s41598-022-19246-w

Baioumy, H., Anuar, M., Adlan, M., Arifin, M. & Al-Kahtany, K. 2020. Source and origin of late Paleozoic dropstones from peninsular Malaysia: First record of Mississippian glaciogenic deposits of Gondwana in Southeast Asia. *Geological Journal* 55(9): 6361-6375. https://doi.org/10.1002/gj.3809

Bakhshayesh, B., Salmasi, F. & Azizi, S. 2023. Optimizing performance of location for horizontal and chimney drainage of earthen slopes retaining walls on stability. *Iranica Journal of Energy and Environment* 14(3): 205-213. https://doi.org/10.5829/ijee.2023.14.03.02

Bell, F. G. 2007. *Engineering geology*. Ed. ke-2. Elsevier, hlm. 1-592. ISBN 0080469523, 9780080469522.

Du, G., Ren, Z., Ren, H., Zhao, X. & Yang, P. 2023. Study on the optimal design of anchor retaining wall earth pressure distribution. https://doi.org/10.3233/atde230487

Frodella, W., Elashvili, M., Spizzichino, D., Gigli, G., Nadaraia, A., Kirkitadze, G. et al. 2021. Applying close-range non-destructive techniques for the detection of conservation problems in rock-carved cultural heritage sites. *Remote Sensing* 13(5): 1040. https://doi.org/10.3390/rs13051040

Guo, J., Wu, Z. & Li, K. 2023. Stability analysis of a soft-hard-interbedded anti-inclined rock slope. *Scientific Reports* 13(1). https://doi.org/10.1038/s41598-023-28657-2

Hamzah, N. & Yusof, N. 2022. Characterization of tropical Kenny Hill weathered sandstone using non-disruptive testing of Pundit and resistivity testing. *Journal of Mechanical Engineering* 19(2): 233-249. https://doi.org/10.24191/jmeche.v19i2.19791

He, Y., Ding, M., Zheng, H., Gao, Z., Huang, T., Duan, Y. & Luo, S. 2023. Integrating development inhomogeneity into a geological disaster risk assessment framework in mountainous areas: A case study in Lushan-Baoxing counties, southwestern China. *Natural Hazards* 117(3): 3203-3229. https://doi.org/10.1007/s11069-023-05983-2

Hoek, E. & Marinos, P. 2007. Brief history of the development of the Hoek-Brown failure criterion. *Soils and Rocks* 2.

Hussin, H., Arifin, M., Rusydy, I. & Ghani, A. 2022. Valuation of rock mass classification and rockfall geohazard in an abandoned limestone quarry for reclamation. https://doi.org/10.21203/rs.3.rs-2020625/v1

Jia, Y., Liu, J., Guo, L., Deng, Z., Li, J. & Zheng, H. 2021. Locomotion of slope geohazards responding to climate change in the Qinghai-Tibetan Plateau and its adjacent regions. *Sustainability* 13(19): 10488. https://doi.org/10.3390/su131910488

Johari, A. et al. 2016. An analytical solution for reliability assessment of pseudo-static stability of rock slopes using the jointly distributed random variables method. *Iranian Journal of Science and Technology: Transactions of Civil Engineering* 39: 351-363.

Lamessa, G. & Meten, M. 2021. Stability analysis of rock slope along selected road sections from Gutane Migiru town to Fincha Sugar Factory, Oromia, Ethiopia. *Applied Sciences* 3(2). https://doi.org/10.1007/s42452-020-04026-w

Li, Q. 2024. Quick extraction of joint surface attitudes and slope preliminary stability analysis: A new method using unmanned aerial vehicle 3D photogrammetry and GIS development. *Remote Sensing* 16(6): 1022. https://doi.org/10.3390/rs16061022

Li, S., Ni, Z., Zhao, Y., Hu, W., Long, Z., Ma, H. et al. 2022. Susceptibility analysis of geohazards in the Longmen Mountain region after the Wenchuan earthquake. *International Journal of Environmental Research and Public Health* 19(6): 3229. https://doi.org/10.3390/ijerph19063229

Liu, C., Liu, X., Xiao-chu, P., Wang, E. & Wang, S. 2019. Application of 3D-DDA integrated with unmanned aerial vehicle-laser scanner (UAV-LS) photogrammetry for stability analysis of a blocky rock mass slope. *Landslides* 16(9): 1645-1661. https://doi.org/10.1007/s10346-019-01196-6

Liu, B., Wang, Z. & Zhong, X. 2021. Particle swarm optimization algorithm in numerical simulation of saturated rock slope slip. *Mathematical Problems in Engineering* 2021: 1-11. https://doi.org/10.1155/2021/6682659

Mao, Y., Chen, L., Nanehkaran, Y., Azarafza, M. & Derakhshani, R. 2023. Fuzzy-based intelligent model for rapid rock slope stability analysis using QSlope. *Water* 15(16): 2949. https://doi.org/10.3390/w15162949

Mohamad, A. G., Mohd R., U., Mohd S., H. & Abdul Ghani, M. R. 2022. Application of Schmidt hammer rebound test for weathering profile classification of granite, Paya Terubong, Penang, Malaysia. *Warta Geologi* 48(1): 23-29.

Nagendran, S., Ismail, M. & Wen, Y. 2019. 2D and 3D rock slope stability assessment using the limit equilibrium method incorporating photogrammetry technique. *Bulletin of the Geological Society of Malaysia* 68: 133-139. https://doi.org/10.7186/bgsm68201913

Obregon, C. & Mitri, H. 2019. Probabilistic approach for open pit bench slope stability analysis: A mine case study. *International Journal of Mining Science and Technology* 29: 629-640.

Ren, Q. & Meng, X. 2022. Study on mechanical response and stability algorithm of soft and hard rock interbedded slope excavation. *Complexity* 2022(1). https://doi.org/10.1155/2022/3331097

Singh, S. K., Banerjee, B. P., Lato, M. J., Sammut, C. & Raval, S. 2022. Automated rock mass discontinuity set characterisation using amplitude and phase decomposition of point cloud data. *International Journal of Rock Mechanics and Mining Sciences* 152. http://dx.doi.org/10.1016/j.ijrmms.2022.105072

Tang, H., Yong, R. & Ez Eldin, M. A. M. 2016. Stability analysis of stratified rock slopes with spatially variable strength parameters: The case of the Qianjiangping landslide. *Bulletin of Engineering Geology and the Environment* 76(3).

Tannant, D. 2015. Review of photogrammetry-based techniques for characterisation and hazard assessment of rock faces. *International Journal of Geohazards and Environment*: 76-87. https://doi.org/10.15273/ijge.2015.02.009

Tuckey, Z. & Paul, J. 2016. Discontinuity survey and brittle fracture characterisation in open pit slopes using photogrammetry. https://doi.org/10.36487/acg_rep/1604_39_tuckey

Wang, S., Zhang, Z., Wang, C., Zhu, C. & Ren, Y. 2019. Multistep rocky slope stability analysis based on unmanned aerial vehicle photogrammetry. *Environmental Earth Sciences* 78(8). https://doi.org/10.1007/s12665-019-8145-z

Zhang, S., Tan, S., Liu, L., Ding, D., Sun, Y. & Li, J. 2023. Slope rock and soil mass movement geological hazards susceptibility evaluation using information quantity, deterministic coefficient, and logistic regression models and their comparison at Xuanwei, China. *Sustainability* 15(13): 10466. https://doi.org/10.3390/su151310466